Journal of Building Engineering 15 (2018) 290–297

Contents lists available at ScienceDirect

Journal of Building Engineering

journal homepage: www.elsevier.com/locate/jobe

Experimental and numerical study on the bearing capacity of soils reinforced using geobags

Nader Hataf*, Mehdi Sayadi

Department of Civil and Environmental Engineering, Shiraz University, Shiraz, Iran

ARTICLE INFO

Keywords:
Geobag
Foundation
Bearing Capacity
Reinforced soil

ABSTRACT

In this study, the soil bearing capacity improvement using geobags is investigated. The bearing capacities of shallow foundations on reinforced and unreinforced soil under vertical loads are determined experimentally and numerically. Different sizes of geobags, as well as number and arrangement of geobags, were used in physical models and the load-settlement curves have been obtained. In the next step, laboratory conditions were simulated employing a 3D finite element computer code. Having validated the numerical modeling, the influence of other factors such as the scale effect on soil improvement and failure mode under a footing are investigated. Results of this study show that using geobags under footings significantly increases the bearing capacity of foundation. It was also found that the number and arrangement of geobags are the most important factors in the increase of bearing capacity and decrease of settlements of foundations.

1. Introduction

Geobags, soilbags; sandbags, etc. are bags usually made from textiles having high tensile strength and filled with materials such as gravel, sand and even construction wastes. Advantages of soil reinforcement by geobags summarized as follows [9]:

(i) Geobags are light.
(ii) Their transportation and relocation are very easy.
(iii) Compatibility with the environment due to no use of any chemicals and there is no noise during construction.
(iv) No special or heavy construction equipment is needed.
(v) The materials inside geobags may be any granular remains and construction wastes such as recycled concrete, asphalt, tire and tile.

Use of geosynthetics and geobags for protection against flood and controlling erosion of river and sea shores, especially sand beaches was known for decades [7,8]. Recently, geobags have found many other applications as temporary and permanent structures in engineering projects. Bearing capacity and settlements of shallow foundations have always been great concerns for engineers and researchers in geotechnical and civil engineering projects. The use of geobags to increase bearing capacity of soft soils is one of these new applications to increase bearing capacity and reduce settlement. Confining the soil by geobag leads to increase in its bearing capacity. This advantage has encouraged the engineers to use geobags for geotechnical improvement of sites with low bearing capacity. Building retaining walls, constructing small temporary buildings, reducing vibrations due to the movement of vehicles and earthquakes are some other applications of geobags.

Hence investigations on geobags behavior are carried out in the last decades worldwide, theoretically, experimentally and numerically. The aim of this study is to investigate the role of geobags in increasing the bearing capacity of soils through a series of experimental and numerical modeling.

2. Previous studies

Chen [4] investigated the geobags' behavior under two-dimensional space. Matsuoka and Liu [9] studied the effect of geobags connections on their bearing capacity by performing a series of experimental tests and found that the bearing capacity increased by connecting geobags horizontally. Aqil et al. [2] investigated the failure mechanism and deformation of overlapping geobags under lateral shear. Tantono and Bauer [11] studied the two-dimensional behavior of geobags. Pu et al. [10] studied the behavior of geobags theoretically. They presented the effect of geobag improvement using the concept of apparent cohesion, C_a. Using Mohr–Coulomb failure criterion for predicting the apparent cohesion and ultimate strength of geobag was employed by following equations:

$$\sigma_{1f} = K_p\sigma_{3f}+2C_a\sqrt{K_p} \rightarrow \sigma_{1f} = 2C_a\sqrt{K_p} \quad (1)$$

* Corresponding author.
E-mail address: nhataf@shirazu.ac.ir (N. Hataf).

https://doi.org/10.1016/j.jobe.2017.11.015
Received 9 September 2016; Received in revised form 19 November 2017; Accepted 20 November 2017
Available online 08 December 2017
2352-7102/ © 2017 Published by Elsevier Ltd.

$$C_a = \frac{K_p \Delta\sigma_3 - \Delta\sigma_1}{2\sqrt{K_p}} \quad (2)$$

In these equations σ_1 and σ_3 are representing stresses in filling soil. σ_{1f} and σ_{3f} are external stresses on geobag, $\Delta\sigma_1$and $\Delta\sigma_3$ are average of excess stresses due to tension in geobag and K_p is Rankine's passive earth pressure coefficient.Yamamoto and Jin [12] obtained a three-dimensional relationship for the stress - strain behavior of geobags. Chew et al. [5] achieved consolidation rate of clay geobags under various tests and compared the results with the one dimensional consolidation theory. Ansari et al. [1] simulated three-dimensional model of geobag numerically and they compared the models with the concluded relationship for geobags in two-dimensional space under static and dynamic vertical loads. Javahari and Hataf [6] simulated the geobags mechanical behavior under vertical load using finite element method numerically. They also studied the behavior of geobags in the three dimensional environment. They developed the following equation to determine the apparent cohesion employing Drucker-Prager yield criterion as follows:

$$c_a = \frac{T}{2R\sqrt{K_p}}\left(\sqrt{d^2 + \frac{4d - 16R/H}{1 - R/H}} + d\right) \quad (3)$$

In this equation, T is the tensile stress developed in bag material, B, L and H are geobag dimensions and $d = \frac{1+\frac{R}{H}}{\frac{1}{3}-\alpha^2} - 4$ and $\frac{1}{R} = \frac{1}{B} + \frac{1}{L} + \frac{1}{H}$.

3. Experimental study

3.1. Materials and apparatus used

In order to perform laboratory model tests a box with dimensions of 1.0 × 1.0 × 1.0 m was used, Fig. 1. The dimensions of the box should be selected in such a way that the boundary conditions do not affect the test results. In other words, the effect of geobag should not continue to the boundaries of the container. For this purpose, an initial analysis using software PLAXIS 3D was performed and the range of induced stresses and displacements around geobag was determined. Floor and two opposite walls of the box were made from steel plates and two other walls were covered by glass with a thickness of 6 mm. To apply static load a servo hydraulic loading system was used. The system has the possibility of applying a controlled pressure stepwise up to 95 kN. Displacement measuring system consisted of 3 LVDTs, data recorder and a computer.

In this study, two foundation models were built from hard plastic having dimensions of 10 × 10 × 4 cm and 15 × 15 × 5 cm. These

Fig. 1. The test box.

Fig. 2. The geobags used.

thicknesses were used to achieve acceptable rigidity.

To make geobag models geotextile sheets were used. In this way, geotextile sheets cut to the required size and then three sides were sewn forming a bag and one side was sewn after filling the bag with soil. Fig. 2 shows geobag physical models.

The soil used was sand its properties are given in Table 1. The geotextile strength parameters are determined according to the standard ASTM D4595-09 [3]. Properties of used geotextile in this study are shown in Table 2.

3.2. Test procedure

The test box was first filled using the sand in 5 layers. Each layer, twenty centimeters thick, was poured by rain method. In all tests, soil was poured from about 15 cm height and to increase unit weight, each sand layer was rammed by dropping a weight from a specified height. To reach the uniform unit weight throughout the box, the amount of energy applied to the entire surface of the soil kept constant in each layer. A standard Proctor hammer and a piece wood, with a dimension of 20 × 20 cm, was used to ram the layers.

Before loading, a small load was applied on the foundation model and displacements were set to zero and then loading was started. Increasing of the loading was considered 2 bars on each stage and each stage continued, till displacement reached a constant amount. Since in some loading experiments, the load limits have not been reached, for a more accurate and detailed examination of the load tolerated by the foundation and a better comparison, the results of the force input into the system at different settlement to the width of the foundation ratio were considered.

4. Numerical study

Similar to the conditions of the tests in the laboratory, numerical

Table 1
The properties of sand used.

D_{10} (mm)	0.065
D_{30} (mm)	0.419
D_{60} (mm)	2.214
Coefficient of uniformity (C_u)	34.06
Coefficient of curvature (C_c)	1.22
Unit weight (kN/m^3)	17.6
Minimum unit weight (kN/m^3)	16.6
Maximum unit weight (kN/m^3)	20.6
e	0.43
e_{min}	0.29
e_{max}	0.59
Cohesion (kPa)	2.1
Friction angle (degree)	32.2

Table 2
Properties of geotextile.

Unit weight (gr/m^2)	670
Tensile strength (kN/m)	15.76
Thickness (mm)	0.6

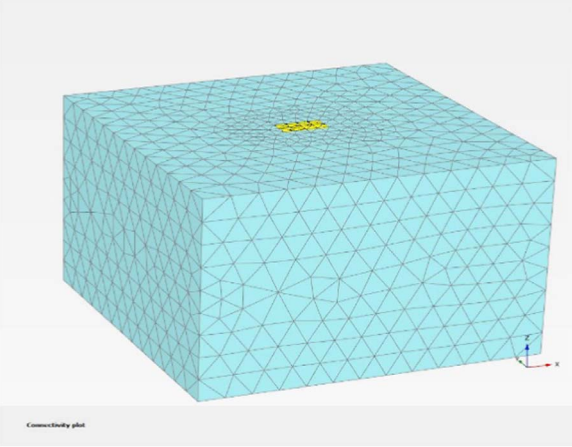

Fig. 3. The 3D modeling created with PLAXIS 3D.

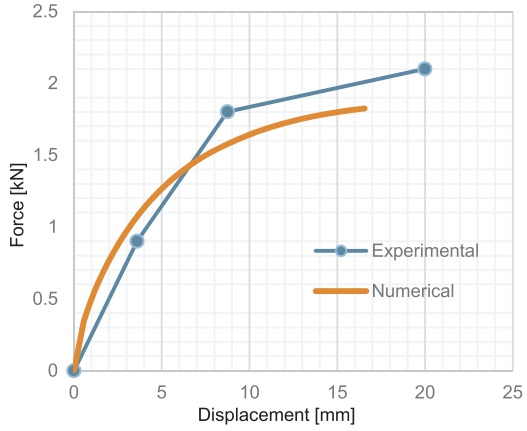

Fig. 4. The force-displacement diagram for experimental and numerical modeling without improvement for foundation model 10 × 10 cm.

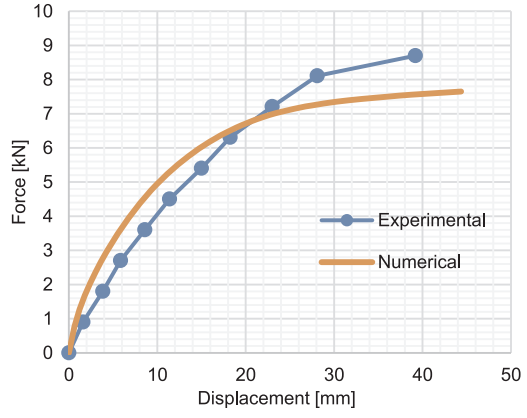

Fig. 5. The force-displacement diagram for experimental and numerical modeling without improvement for foundation model 15 × 15 cm.

models were made using PLAXIS 3D finite element software. Numerical simulation was performed with actual dimensions, afterwards. For the simulation of the tests, soil and dimensions are considered the same as

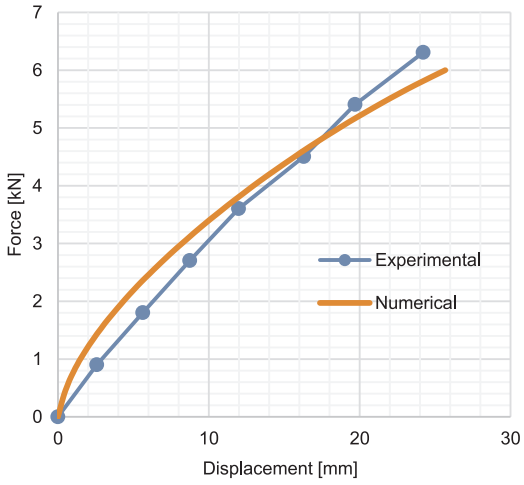

Fig. 6. The force-displacement for experimental and numerical modeling by a geobag with dimensions 15 × 15 × 4 cm under foundation model 10 × 10 cm.

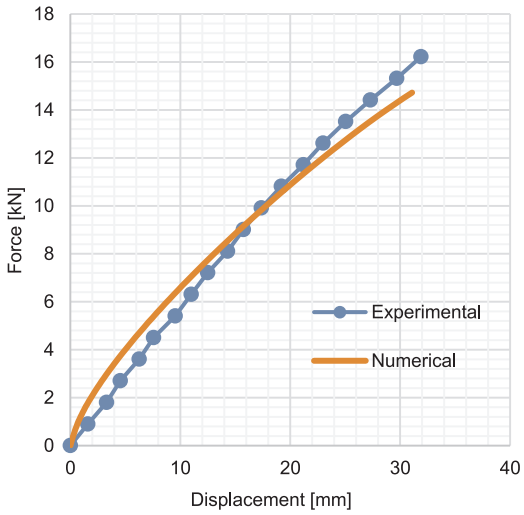

Fig. 7. The force-displacement diagram for experimental and numerical modeling by a geobag with dimensions 20 × 20 × 5 cm under foundation model 15 × 15 cm.

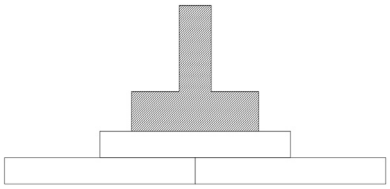

Fig. 8. The schematic view of the arrangement of three geobags.

the those in experimental tests. The elastic-perfectly plastic Mohr-Coulomb soil model was utilized for simulation of soil behavior. The standard boundary conditions (i.e. total fixity at the bottom and horizontal fixities at the sides of the model) were defined. Interface element was used for the contact surfaces between soil and geo-bags. The model used for foundation was linear elastic and impenetrable with drained conditions. To simulate the geobag model, a soil with the corresponding geotextile characteristics used in the construction of geobags has been used. Triangular elements were used for meshing of 10 nodes and medium sizes. To select the mesh size, mesh sensitivity analysis was conducted and finally the suitable mesh size was selected. The model analysis was done in two phases. In the initial phase, the total soil volume and geobag models are considered. In the next phase, the foundation and loading model was activated. Fig. 3 shows one of

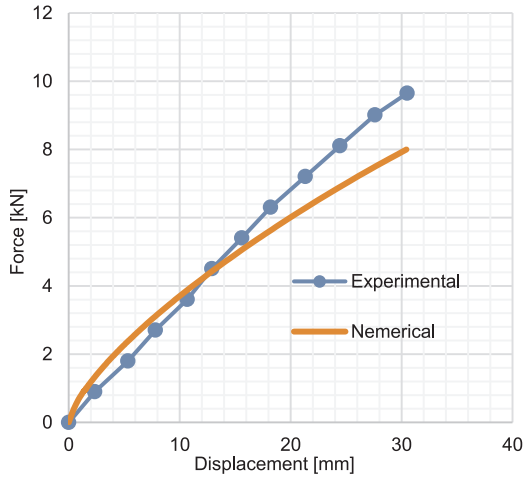

Fig. 9. The force-displacement diagram for experimental and numerical modeling using three geobags (first arrangement) with dimensions of 15 × 15 × 4 cm under foundation 10 × 10 cm.

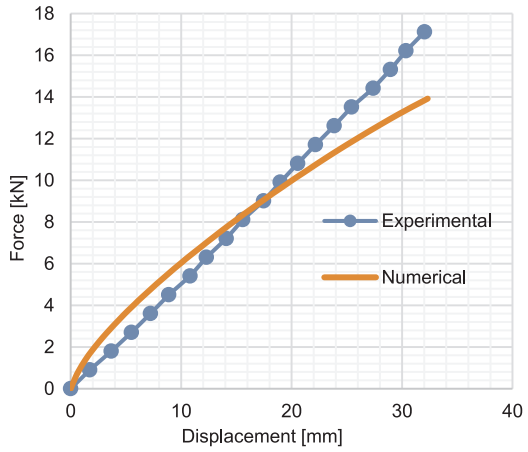

Fig. 10. The force-displacement diagram for experimental and numerical modeling using three geobags (first arrangement) with dimensions of 20 × 20 × 5 cm under foundation 15 × 15 cm.

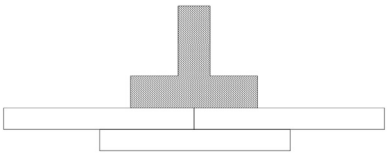

Fig. 11. The schematic view of second arrangement using three geobags.

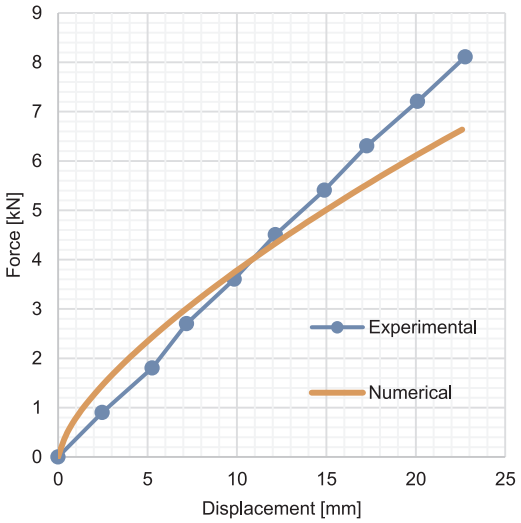

Fig. 12. The force-displacement diagram for experimental and numerical modeling of three geobags (second arrangement) with dimensions of 15 × 15 × 4 cm under foundation 10 × 10 cm.

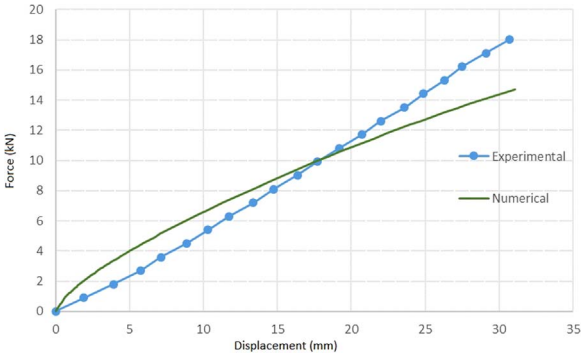

Fig. 13. The force-displacement diagram for experimental and numerical modeling of three geobags (second arrangement) with dimensions of 20 × 20 × 5 cm under foundation 15 × 15 cm.

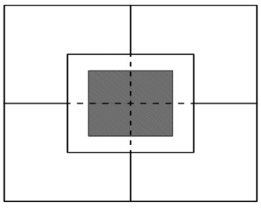

Fig. 14. The schematic view of first arrangement five geobags.

the models made using this software.

5. The experimental and numerical test results

Since the aim of this study was to determine the effect of using geobag in bearing capacity improvement, it was necessary to investigate the behavior of the unreinforced soil, first. Afterwards, soil bags were used and the results of experimental and numerical modeling were compared. The loading for both improved soil and soil without improvement continued until one of these condition has reached:

i) The bearing capacity or the maximum soil pressure corresponding to shear failure has been encountered and/or

ii) The settlement failure occurred which was defined as the settlement value equal or greater than 0.2B, where B is the foundation width.

This criterion was used both in laboratory testing and numerical modeling therefore the comparison between test results and analytical results can be conducted.

5.1. Bearing capacity of unreinforced soil

Tests were performed to determine the bearing capacity of unreinforced soil using two foundation models with dimensions of 10 × 10 cm and 15 × 15 cm. Figs. 4 and 5 show force-displacement diagrams of experimental and numerical models, respectively.

5.2. Bearing capacity of the soil improved using geobags

In the next step, a geobag with dimensions of 15 × 15 × 4 cm was embeded exactly under 10 × 10 cm foundation model and a geobag with dimensions of 20 × 20 × 5 cm embeded exactly under foundation model 15 × 15 cm.

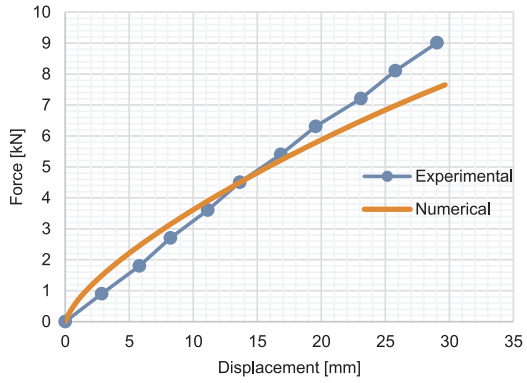

Fig. 15. The force-displacement diagram for experimental and numerical modeling of five geobags (first arrangement) with dimensions of 15 × 15 × 4 cm under foundation model 10 × 10 cm.

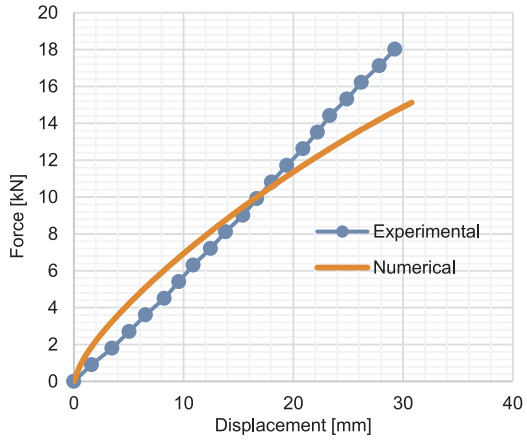

Fig. 16. The force-displacement diagram for experimental and numerical modeling of five geobags (first arrangement) with dimensions of 20 × 20 × 5 cm under foundation 15 × 15 cm.

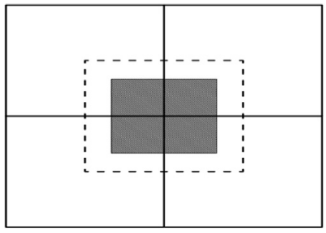

Fig. 17. The schematic view of second arrangement five geobags.

Figs. 6 and 7 show force-displacement diagram for experimental and numerical modeling by geobag under 10 × 10 cm and 15 × 15 cm foundation, respectively.

To investigate the effect of the number of geobags on increasing the bearing capacity, more geobags were used. Therefore, in the first step, three geobags with dimensions of 15 × 15 × 4 cm under 10 × 10 cm foundation model and three geobags with dimensions of 20 × 20 × 5 cm under 15 × 15 cm foundation model were used. Arrangement of geobags in this test is shown in Fig. 8, schematically.

The force-displacement diagrams for these tests under foundation models of 10 × 10 and 15 × 15 cm shown in Figs. 9 and 10, respectively.

To investigate the effect of arrangement of geobags on soil improvement the arrangement was changed so that two bags are located beneath the foundation and the other geobag below these two geobags, Fig. 11.

The force-displacement diagrams of the results of these tests for foundation models 10 × 10 and 15 × 15 cm are shown in Figs. 12 and 13, respectively.

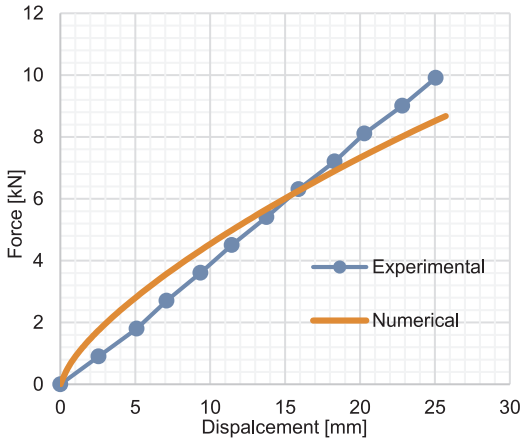

Fig. 18. The force-displacement diagram for experimental and numerical modeling of five geobags (second arrangement) with dimensions of 15 × 15 × 4 cm under foundation 10 × 10 cm.

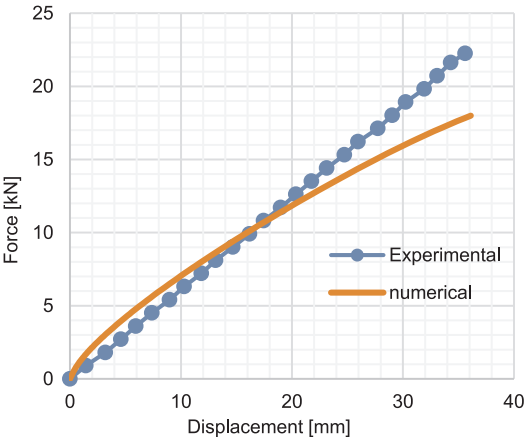

Fig. 19. The force-displacement diagram for experimental and numerical modeling of five geobags (second arrangement) with dimensions of 20 × 20 × 5 cm under foundation 15 × 15 cm.

Table 3
The R_{mB} for various displacement under foundation model 10 × 10 cm.

Soil condition	$R_{0.05B}$	$R_{0.10B}$	$R_{0.15B}$	$R_{0.20B}$	$R_{0.25B}$
Unreinforced soil	1.00	1.00	1.00	1.00	1.00
Reinforced using one geobag	1.41	1.66	2.1	2.51	2.73
Reinforced using three geobags (first arrangement)	1.48	1.84	2.59	3.13	3.52
Reinforced using three geobags (second arrangement)	1.50	1.99	2.71	3.29	3.72
Reinforced using five geobags (first arrangement)	1.36	1.77	2.43	2.95	3.34
Reinforced using five geobags (second arrangement)	1.53	2.11	2.95	3.66	4.21

In the next step, the number of geobags was increased to five. For this purpose, one geobag was used beneath the foundation and four other geobags were placed below this geobag, Fig. 14.

The force-displacement diagrams for these tests under 10 × 10 cm foundation model and 15 × 15 cm are shown in Figs. 15 and 16, respectively.

In order to investigate the effect of the arrangement, placement of geobags was changed, so that four geobags was placed beneath foundation and one other geobag below them, Fig. 17.

Table 4
The ratio of R_{mB} at various displacement under foundation model 15 × 15 cm.

Soil condition	$R_{0.05B}$	$R_{0.10B}$	$R_{0.15B}$	$R_{0.20B}$	$R_{0.25B}$
Unreinforced soil	1.00	1.00	1.00	1.00	1.00
Reinforced using one geobag	1.37	1.58	1.74	1.87	2.07
Reinforced using three geobags (first arrangement)	1.17	1.44	1.69	1.97	2.3
Reinforced using three geobags (second arrangement)	1.17	1.53	1.81	2.13	2.57
Reinforced using five geobags (first arrangement)	1.28	1.64	1.94	2.23	2.64
Reinforced using five geobags (second arrangement)	1.41	1.7	1.97	2.27	2.68

The force-displacement diagrams for these tests under foundation 10 × 10 cm and foundation 15 × 15 are shown in Figs. 18 and 19, respectively.

6. Analysis and discussion of the results

6.1. The results of experimental tests

At first, the results of the tests under the 10 × 10 cm foundation model are discussed. Then the tests under the 15 × 15 cm foundation model are reviewed. In the end the results of both foundation models are compared with each other.

6.1.1. Results and analysis of the tests on 10 × 10 cm foundation model

Since in some of the tests, loading did not reached to the ultimate bearing load, for more accurate investigation and comparison, the loads borne by the foundation model were calculated at different displacements and shown in Table 3. A parameter, R_{mB}, is defined as follows for this purpose:

$$R_{mB} = \frac{\textbf{The load born eat displacement of mB for reinforced soil}}{\textbf{The load born eat displacement of mB for unreinforced soil}}$$

Table 3 shows the R_{mB} for various displacements levels.

As shown in Table 3, the use of geobags improves the bearing capacity of the shallow foundations. This is because of the confining effect of bags which causes the soil bears a higher vertical stress. The amount of increase in bearing capacity, however, for low displacement (i.e. 0.05B) is small with a maximum of 53% in improvement mode by five geobags. This is evident at the beginning of loading because the amount of load on the foundation model was low. The amount of the increase for larger displacement of different improvement modes can be observed. On the other hand, during the loading geobag behaves as part of the foundation and this behavior explains further the increase in bearing capacity. The same behavior can be seen for other number of geobags.

6.1.2. Results and analysis of the tests under foundation model 15 × 15 cm

Table 4 shows R_{mB} ratio for 15 × 15 cm foundation at various displacement levels.

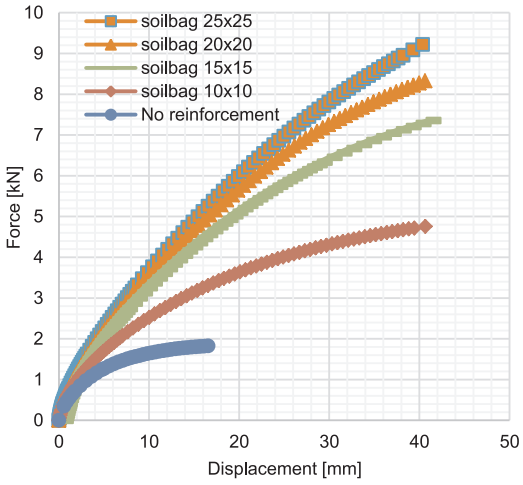

Fig. 20. The force-displacement diagram effect of geobag dimensions on improvement.

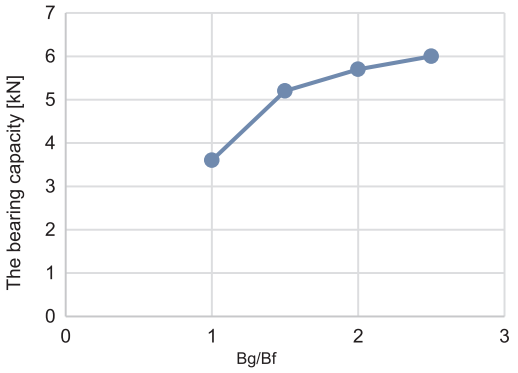

Fig. 21. The diagram the effect of geobag dimensions on the bearing capacity.

Fig. 22. The typical arrangement of the improvement using 5 geobags.

According to Table 4, it can be seen that the trend of the increase in bearing capacities for 15 × 15 cm foundations is almost the same as for the 10 × 10 cm foundation model. However, it can be seen that the amount of the increase in bearing capacity under 10 × 10 cm foundation model is more than that for foundation model 15 × 15 cm. The reasons for this can be attributed to soil failure mode under foundation model, which means that under 10 × 10 cm foundation model punch

Table 5
The bearing capacity of numerical modeling.

Soil condition	The percent of error under foundation model 10 × 10	The percent of error under foundation model 15 × 15
Unreinforced soil	15.60	11.02
Reinforced using one geobag	4.20	6.41
Reinforced using three geobags (first arrangement)	11.42	16.70
Reinforced using three geobags (second arrangement)	14.76	18.04
Reinforced using five geobags (first arrangement)	8.41	19.24
Reinforced using five geobags (second arrangement)	7.40	13.56

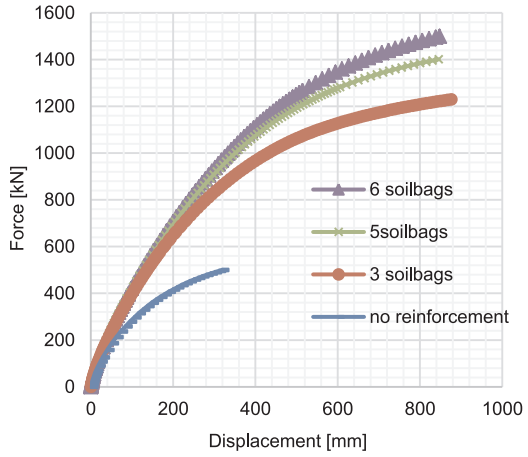

Fig. 23. The force-displacement diagram of numerical modeling in real dimension.

Table 6
The bearing capacity ratio of models with real dimensions.

Soil conditions	$R_{0.2B}$
Unreinforced soil	1.00
Reinforced using 3 geobags	1.56
Reinforced using 5 geobags	1.67
Reinforced using 6 geobags	1.71

failure occurred and improvement by geobag lead to increase the bearing capacity considerably. Another reason for the difference of the increased in bearing capacity between two foundation model can be attributed to the ratio of the geobag surface to the foundation area. This means that, the ratio under the 10 × 10 cm foundation model is 2.25 and is 1.78 for 15 × 15 cm foundation.

6.2. The results of numerical modeling

All most the same trend as for experimental results were observed in numerical modeling.

To compare the results of numerical and experimental modeling, error percent of the numerical bearing capacity with respect to the experimental bearing capacity at $R_{0.2B}$ were calculated and shown in the Table 5. According to Table 5, maximum and minimum of the error percent is 19% and 4.2%, respectively. So we can conclude that numerical modeling can predict the behavior of improved foundation by geobag acceptably.

6.3. The effect of geobag dimensions

In this section, the effect of dimensions of geobags on the bearing capacity was investigated. For this purpose, the foundation model dimensions are kept constant and the geobag dimensions were changed. Geobags dimensions 10 × 10, 15 × 15, 20 × 20 and 25 × 25 cm were selected for modeling. The force-displacement diagrams of the performed modeling are shown together in Fig. 20. for comparison.

In order to show the effect of geobag dimensions on improvement, the bearing capacities at displacements of 0.2B levels are drawn against the B_g/B_f (geobag width to foundation width) ratio, Fig. 21. As it can be seen from both figures the increase in B_g/B_f causes an increase in bearing capacity. However, with increase of ratio $\mathbf{B_g/B_f}$ the slope of the curve, Fig. 21, is reduced. It means that with increasing the ratio of geobag width to foundation width, amount of the increase in bearing capacity reduces.

6.4. Scale effect in soil reinforcement

After validation of the numerical results using the experimental results, large scale numerical geobag models were made. Properties of soil used in the actual size modeling, was identical to those used in experimental modeling. In this modeling the foundation model dimensions of 1.0 × 1.0 × 0.1 m, the geobag model dimensions of 1.2 × 0.5 × 0.2 m considered. At first, such as the previous models, modeling is started with unreinforced soil. In the next step, the improvement made using 3, 5 and 6 geobags were performed as shown in Fig. 22.

To illustrate the effect of improvement by large scale geobags, the force-displacement diagrams of all performed modeling are shown together in Fig. 23.

The load born at of 0.2B displacement level was considered for comparison in all cases. The amount of the bearing capacity ratio, $R_{0.2B}$, for numerical modeling with real dimensions are shown in Table 6. As it can be seen the amount of improvement of bearing capacity is significant and increases with the increase in the number of geobags.

6.5. Failure zone beneath foundation

In this section, failure zones beneath the foundation models obtained numerically are compared for cases cited in previous sections. First, failure zones beneath foundation model with dimensions 10 × 10 cm for unreinforced and reinforced soil using geobag of 15 × 15 cm are shown in Fig. 24.

By comparing these failure zones it can be seen that the width and depth of stressed area for reinforced soil by geobag is smaller than that for unreinforced soil which causes increase in bearing capacity and decrease of settlement of reinforced soil under the same condition with respect to unreinforced soil.

7. Conclusion

The results of this study can be summarized briefly as follows:

1. External force induced a tensile force in bags and this leads to soil confinement and therefore increases te compressive strength of soil reinforced using geobags.
2. Improvement using geobags leads to reduce the settlement of foundation.
3. Increasing the number of geobags causes increase in bearing

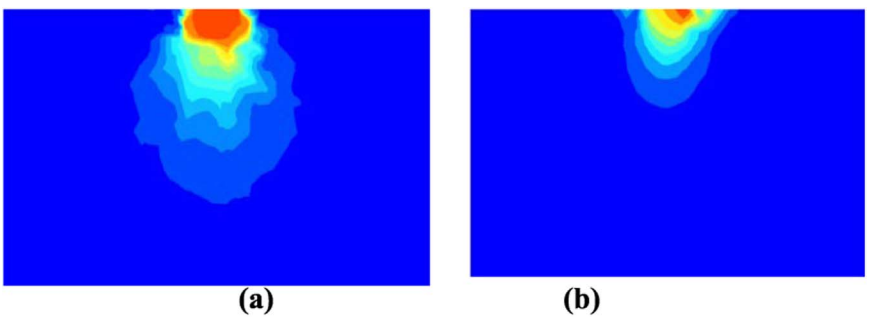

Fig. 24. The failure zone beneath foundation model with dimensions of 15 × 15 cm; (a) The failure zone unreinforced soil; (b) The failure zone for reinforced soil using geobag.

capacity of foundation.

4. Arrangement of geobags under the foundation is an important factor in soil improvement.

References

[1] Y. Ansari, R. Merifield, H. Yamamoto, D. Sheng, Numerical analysis of soilbags under compression and cyclic shear, Comput. Geotech. 38 (5) (2011) 659–668.

[2] U. Aqil, K. Matsushima, Y. Mohri, S. Yamazaki, F. Tatsuoka, Application of stacked soil bags to repair and maintenance works of small earth dams, Nogyo Doboku Gakkai Taikai Koenkai koen Yoshishu 2006 (2006) 592–593.

[3] ASTM D4595-09. Standard test method for tensile properties of geotextiles by the wide-width strip method, American Society for Testing and Materials, West Conshohocken, Pennsylvania, USA.

[4] Y. Chen, Deformation and Strength Properties of a 2D Model Soilbag and Design Method of Earth Reinforcement by Soilbags. Report to Venture Business Laboratory, Nagoya Institute of Technology, 1999 (in Japanese).

[5] S.H. Chew, P.Y. Pang, C.Y. Tan, K.E. Chau, Laboratory study on the consolidation settlement of clay-filled geotextile tube and bags, J. Geoengin. 6 (1) (2011) 41–45.

[6] M. Javahari, N. Hataf, Numerical investigation of 3-D behavior of geobag under distributed vertical load. Proceedings of the first Iranian Conference on Geotechnical Engineering, Ardabil, Iran, 2013.

[7] R. Karpurapu, The geosynthetics for sustainable construction of infrastructure projects, Indian Geotech. J. 47 (1) (2017) 2–34.

[8] H. Kim, M. Won, K. Lee, J.C. Jamin, Model tests on dredged soil–filled geocontainers used as containment dikes for the saemangeum reclamation project in South Korea, Int. J. Geomech. 16 (2) (2016).

[9] H. Matsuoka, S. Liu, New earth reinforcement method by soil-bags (DONOW), Soils Found. 43 (6) (2003) 173–188.

[10] Minyan Pu, Liu Sihong, Zhu Kesheng, Experimental Study on an Expansive Soil and its Containment in Bags Under Drying-wetting Cycles, College of Water Conservancy and Hydropower Engineering, Hohai University, Nanjing, 2008 (in Chines).

[11] S.F. Tantono, E. Bauer. Numerical simulation of a soilbag under vertical compression, in: Proceedings of the 12th International Conference of International Association for Computer Methods and Advanced in Geomechanics (IACMAG), Goa. India, 1–6 October 2008, pp. 433–439.

[12] H. Yamamoto, S. Jin, Model tests on bearing capacity of soil-bags, in: Challenges, Opportunities and Solutions in Structural Engineering and Construction, 2010, pp. 987–992.